

Published in final edited form as:

*Exp Neurol.* 2011 January ; 227(1): 96–103. doi:10.1016/j.expneurol.2010.09.017.

## Characterization of the Brain Injury, Neurobehavioral Profiles and Histopathology in a Rat Model of Cerebellar Hemorrhage

Tim Lekic<sup>a</sup>, William Rolland<sup>a</sup>, Richard Hartman<sup>b</sup>, Joel Kamper<sup>b</sup>, Hidenori Suzuki<sup>a</sup>, Jiping Tang<sup>a</sup>, and John H. Zhang<sup>a,c,d,\*</sup>

<sup>a</sup>Department of Physiology, School of Medicine, Loma Linda University, Loma Linda, Calif.

<sup>b</sup>Department of Psychology, School of Science and Technology, Loma Linda, Calif.

<sup>c</sup>Department of Anesthesiology, School of Medicine, Loma Linda University, Loma Linda, Calif.

<sup>d</sup>Department of Neurosurgery, School of Medicine, Loma Linda University, Loma Linda, Calif.

### Abstract

Spontaneous cerebellar hemorrhage (SCH) represents approximately 10% of all intracerebral hemorrhage (ICH), and is an important clinical problem of which little is known. This study stereotaxically infused collagenase (type VII) into the deep cerebellar paramedian white matter, which corresponds to the most common clinical injury region. Measures of hemostasis (brain water, hemoglobin assay, Evans blue, collagen-IV, ZO-1, and MMP-2 and MMP-9) and neurodeficit were quantified twenty-four hours later (Experiment 1). Long-term functional outcomes were measured over thirty days using the ataxia scale (modified Luciani), open field, wire suspension, beam balance and inclined plane (Experiment 2). Neurocognitive ability was assessed on the third week using the rotarod (motor learning), T-maze (working memory) and water-maze (spatial learning and memory) (Experiment 3), followed by a histopathological analysis one week later (Experiment 4). Stereotaxic collagenase infusion caused dose-dependent elevations in brain edema, neurodeficit, hematoma volume and blood-brain barrier rupture, while physiological variables remained stable. Most functional outcomes normalized by third week, while neurocognitive testing showed deficits parallel to the cystic-cavitary lesion at thirty days. All animals survived until sacrifice, and obstructive hydrocephalus did not develop. These results suggest that the model can generate important translational information about this subtype of ICH, and could be used for future investigations of therapeutic mechanisms after cerebellar hemorrhage.

### Keywords

cerebellar hemorrhage; neurobehavioral testing; histopathology; rats

---

© 2010 Elsevier Inc. All rights reserved.

\*Corresponding author: John H. Zhang, MD, PhD, Department of Physiology, Loma Linda University School of Medicine, Risley Hall, Room 223, Loma Linda, California 92354, USA, johnzhang3910@yahoo.com (J.H. Zhang). Tel: 909-558-4723, Fax: 909-558-0119.

**Publisher's Disclaimer:** This is a PDF file of an unedited manuscript that has been accepted for publication. As a service to our customers we are providing this early version of the manuscript. The manuscript will undergo copyediting, typesetting, and review of the resulting proof before it is published in its final citable form. Please note that during the production process errors may be discovered which could affect the content, and all legal disclaimers that apply to the journal pertain.

The authors report no conflicts of interest.

## 1. Introduction

Spontaneous (non-traumatic) cerebellar hemorrhage (SCH) results from the rupture of blood vessels within the cerebellum. SCH is a type of intracerebral hemorrhage (ICH) with an incidence of 1 in 33000 people every year, and accounts for 200,000 (10%) of around 2 million worldwide ICHs (Flaherty et al., 2005; Qureshi et al., 2009). Uncontrolled hematoma expansion causes abrupt ataxic neurological deterioration in nearly half of initially alert hospitalized patients (Rosenberg and Kaufman, 1976; St Louis et al., 1998) leading to a 40% mortality rate despite contemporary imaging and surgical methods (Flaherty et al., 2006; Hill and Silver, 2001). Almost 50% of these survivors will retain some cognitive deficits across motor-learning and visuospatial domains (Baillieux et al., 2008; Dolderer et al., 2004; Kelly et al., 2001; Strick et al., 2009).

The pathophysiological basis of SCH is poorly understood despite surgical approaches that presently diverge from all other forms of ICH (Jensen and St Louis, 2005; Mendelow and Unterberg, 2007); and this underscores the need for translational research (NINDS, 2005). Our preliminary report demonstrated the feasibility of collagenase-induced *intracerebellar* hemorrhage (Lekic et al., 2008). We had used a modification of an established (basal ganglia) ICH model (Rosenberg et al., 1990) that circumvented the hematoma dissections outside rodent cerebella which had complicated autologous blood injection approaches in this brain region previously (Cossu et al., 1991; Cossu et al., 1994).

While each experimental approach possesses drawbacks, the strength of collagenase-induced ICH resides with therapeutic investigations of hemostasis, neurobehavior, and histopathology (Andaluz et al., 2002; Foerch et al., 2008; Hartman et al., 2009; MacLellan et al., 2008; Rosenberg et al., 1990; Thiex et al., 2004). Therefore this study hypothesized that a rodent model of stereotaxic collagenase infusion could be used for translational purposes to extend the pathophysiological understanding of hematoma growth, brain edema, neurological deficit and brain atrophy after cerebellar hemorrhage (Baillieux et al., 2008; Dolderer et al., 2004; Kelly et al., 2001; Rosenberg and Kaufman, 1976; St Louis et al., 1998; Strick et al., 2009).

## 2. Materials and Methods

### 2.1 The Animals and Operative Procedure

Ninety-six adult male Sprague-Dawley rats (290–345g; Harlan, Indianapolis, IN) were used. All procedures were in compliance with the *Guide for the Care and Use of Laboratory Animals* and approved by the Animal Care and Use Committee at Loma Linda University. Aseptic technique was used for all surgeries. Rats were anesthetized with isoflurane (4% induction, 2% maintenance, 70% N<sub>2</sub>O and 30% O<sub>2</sub>) and secured prone onto a stereotaxic frame (Kopf Instruments, Tujunga, CA) before making an incision over the scalp. The following stereotaxic coordinates were then measured from bregma, to locate the deep cerebellar (paramedian) white matter tract: 11.6 mm (caudal), 2.4 mm (lateral), and 3.5 mm (deep). A borehole (1 mm) was drilled, and then a 27-gauge needle was inserted. Collagenase type VII (0.2 U/ $\mu$ L, Sigma, St Louis, MO) was infused by microinfusion pump (rate=0.2  $\mu$ L/min, Harvard Apparatus, Holliston, MA). The syringe remained in place for 10 minutes to prevent back-leakage before being withdrawn. Then the borehole was sealed with bone wax, incision sutured closed, and animals allowed to recover. Control surgeries consisted of needle insertion alone. A thermostat-controlled heating blanket maintained the core temperature (37.0 $\pm$ 0.5°C) throughout the operation. The animals were given free access to food and water upon recovery from anesthesia.

## 2.2 Experiment 1: Early Brain Injury at 24 Hours

**2.2.1 Brain Water Content**—Water content was measured using the wet-weight/ dry-weight method (Tang et al., 2004). Quickly after sacrifice the brains were removed and tissue weights were determined before and after drying for 24 hours in a 100°C oven, using an analytical microbalance (model AE 100; Mettler Instrument Co., Columbus, OH) capable of measuring with 1.0µg precision. The data was calculated as the percentage of water content: (wet weight – dry weight)/wet weight × 100.

**2.2.2 Neuroscore**—The composite neuroscore is a value of sensorimotor function consisting of the combined averages from wire suspension, beam balance and inclined plane (Colombel et al., 2002; Fernandez et al., 1998). The ataxic neuroscore is a modification of the Luciani scale, a summation of scores (maximum=9) measuring: body tone, limb-extension, and dyscoordination (Baillieux et al., 2008). Values are expressed as percent of sham; further details are provided (Experiment 2) below.

**2.2.3 Animal Perfusion and Tissue Extraction**—Animals were fatally anesthetized with isoflurane (≥%5) followed by cardiovascular perfusion with ice-cold PBS for the hemoglobin and Evans blue assays, and immunoblot analyses. The cerebella were then dissected and snap-frozen with liquid-nitrogen and stored in –80°C freezer, before spectrophotometric quantifications or protein extraction.

**2.2.4 Hemorrhagic Volume**—The spectrophotometric hemoglobin assay was performed as previously described (Tang et al., 2004), where extracted cerebellar tissue was placed in glass test tubes with 3 mL of distilled water, then homogenized for 60 seconds (Tissue Miser Homogenizer; Fisher Scientific, Pittsburgh, PA). Ultrasonication for 1 minute lysed erythrocyte membranes, then centrifuged for 30 min, and Drabkin's reagent was added (Sigma-Aldrich) into aliquots of supernatant which reacted for 15 min. Absorbance, using a spectrophotometer (540 nm; Genesis 10uv; Thermo Fisher Scientific, Waltham, MA), was calculated into hemorrhagic volume on the basis of a standard curve (Choudhri et al., 1997).

**2.2.5 Physiological Variables and Vascular Permeability**—Under general anesthesia (operatively), the right femoral artery was catheterized for physiological variables, and re-assessed 24 hours later on the left side, followed by 2% intravenous Evans blue injection (5 mL/kg; 1 hr circulation). Extracted cerebellar tissue was weighed, homogenized in 1 mL PBS, then centrifuged for 30 minutes. After which 0.6 mL of the supernatant was added with equal volumes of trichloroacetic acid, followed by overnight incubation and re-centrifugation. The final supernatant underwent spectrophotometric quantification (615 nm; Genesis 10uv; Thermo Fisher Scientific, Waltham, MA) of extravasated dye, as described (Saria and Lundberg, 1983).

**2.2.6 Western Blotting**—As routinely done (Tang et al., 2004), the concentration of protein was determined using DC protein assay (Bio-Rad, Hercules, CA). Samples were subjected to SDS-PAGE, then transferred to nitrocellulose membrane for 80 minutes at 70 V (BioRad). Blotting membranes were incubated for 2 hours with 5% nonfat milk in Tris-buffered saline containing 0.1% Tween 20 and then incubated overnight with the following primary antibodies: anti-collagen IV (1:500; Chemicon, Temecula, CA), anti-zonula occludens (ZO)-1 (1:500; Invitrogen Corporation, Carlsbad, CA), anti-matrix metalloproteinase (MMP)-2 and anti-matrix metalloproteinase (MMP)-9 (1:1500; Millipore, Billerica, MA). Followed by incubation with secondary antibodies (1:2000; Santa Cruz Biotechnology) and processed with ECL plus kit (Amersham Bioscience, Arlington Heights, Ill). Images were analyzed semiquantitatively using Image J (4.0, Media Cybernetics, Silver Spring, MD).

### 2.3 Experiment 2: Functional Outcome over Thirty Days

Animals were assessed with a battery of tests. The modified Luciani scale (3=severe, 2=moderate, 1=mild, 0=none) was a summation of scores (maximum=9) given for (a) decreased body tone, (b) ipsilateral limb-extensions, and (c) dyscoordination (Baillieux et al., 2008). For locomotion, the path length in open-topped plastic boxes (49cm-long, 35.5cm-wide, 44.5cm-tall) was digitally recorded for 30 minutes and analyzed by Noldus Ethovision tracking software (Hartman et al., 2009). For sensorimotor function, the falling latency was recorded (60 second cut-off) when all four limbs animals were placed perpendicularly onto a stationary horizontal beam balance (50cm-length, 5cm-diameter) or as the forelimbs grasped onto the wire suspension (40cm-length, 3mm-diameter) (Colombel et al., 2002). The inclined plane consisted of a box (70cm-long, 20cm-wide, 10cm-tall) with an analog protractor and hinged base, elevated at 5 degree intervals until the animal slipped backwards (Fernandez et al., 1998).

### 2.4 Experiment 3: Neurocognitive Assessment at Third Week

Higher-order brain function was assessed using several different tests. For the rotarod task, a motor-learning paradigm was assessed by comparing pre-operative performance with four daily blocks on the third week after injury at days 21, 23, 25, and 27 (Hartman et al., 2009; Lekic et al., 2010). The apparatus consisted of a horizontal rotating cylinder (7cm-diameter  $\times$  9.5cm-wide, acceleration= 2 rpm/ 5 sec) requiring continuous walking to avoid falling, which was recorded by photobeam-circuit (Columbus Instruments). The T-Maze assessed short-term (working) memory (Hughes, 2004). Rats were placed into the stem (40 cm  $\times$  10 cm) of a maze and allowed to explore until one arm (46 cm  $\times$  10 cm) was chosen. From the sequence of ten trials, of left and right arm choices, the rate of spontaneous alternation (0% = none and 100% = complete, alternations/ trial) was calculated (Fathali et al., 2010; Zhou et al., 2009). For the Morris water-maze task, spatial learning and memory was assessed over four daily blocks on days 22, 24, 26 and 28 (Hartman et al., 2009; Lekic et al., 2010). The apparatus consisted of a metal pool (110cm diameter), filled to within 15cm of the upper edge, with a platform (11cm diameter) for the animal to escape onto that changed location for each block (maximum=60sec /trial), and digitally analyzed by Noldus Ethovision tracking software. Cued trials measured place learning with the escape platform visible above water. Spatial trials measured spatial learning with the platform submerged and probe trials measured spatial memory once the platform was removed.

### 2.5 Experiment 4: Histopathological Analysis

Thirty days after collagenase infusion, the animals were fatally anesthetized with isoflurane ( $\geq 5\%$ ) followed by cardiovascular perfusion with ice-cold PBS and 10% paraformaldehyde. Brains were removed and postfixed in 10% paraformaldehyde then 30% sucrose (weight/volume) for 3 days. For all neuropathological analyses 10 $\mu$ m thick coronal sections were cut every 500  $\mu$ m caudally on a cryostat (Leica Microsystems LM3050S), then mounted on poly-L-lysine-coated slides and stained. Morphometric analysis of cresyl violet slides involved computer-assisted (ImageJ 4.0, Media Cybernetics, Silver Spring, MD) hand delineation of the ventricles (lateral, third, cerebral aqueduct, and fourth), brainstem, cerebellum (ipsilateral and contralateral), cerebellar layers (white matter, molecular and granular) and lesioned area (cavity, cellular debris). Borderlines were based on criteria defined from stereologic studies using optical dissector principles (Andersen et al., 1992; Korbo et al., 1993; Oorschot, 1996). Brain volumes were calculated with established protocols: (Average [(Area of coronal section) - (lesion area)]  $\times$  Interval  $\times$  Number of sections) (Lekic et al., 2010; MacLellan et al., 2008). Purkinje cells were blindly counted in the viable (non-lesioned) brain tissues in accordance with standard technique (Schmidt et al., 2007; Song et al., 2007). To account for variant Purkinje densities in different folia, these neurons were counted at 200X magnification in fifteen representative areas (500  $\mu$ m  $\times$  500

$\mu\text{m}$  grids) per cerebellar hemisphere of the section with maximal hematoma diameter (Lekic et al., 2010). These measurements were twice repeated, averaged and expressed as the relative number of neurons per millimeter (mm) of folia.

## 2.6 Statistical Analysis

Statistical significance was considered at  $P < 0.05$ . Data was analyzed using analysis of variance (ANOVA), with repeated-measures (RM-ANOVA) for long-term neurobehavior. Significant interactions were explored with conservative Scheffe *post hoc* test, T-test (unpaired) and Mann-Whitney rank sum test when appropriate.

## 3. Results

### 3.1 Experimental Model of Cerebellar Hemorrhage

Systemic physiological variables were stable during and after the surgical procedure (see Table). Within 30 minutes after awakening from anesthesia, the collagenase infused animals exhibited ataxic gaits, ipsilateral limb extensions and decreased body tone. Pathological examinations at 24 hours revealed right cerebellar hemispheric hematomas surrounded with vasogenic edema, without subarachnoid or subdural bleeding and without ventricular obstruction, in spite of substantial amounts of bleeding (Fig. 1B and 1C). All animals survived through the end of the study and obstructive hydrocephalus did not develop.

### 3.2 Experiment 1: Early Brain Injury at 24 Hours

Unilateral collagenase infusion led to dose-dependent elevations of brain water, sensorimotor (composite neuroscore) deficit, hematoma volume, and vascular permeability ( $P < 0.05$ , Fig. 2A–D). Immunoblots show significant elevation of MMP-2 and -9, and degradation of collagen-IV and ZO-1 ( $P < 0.05$ , Fig. 2E).

### 3.3 Experiment 2: Functional Outcome over Thirty Days

Infusion of collagenase (0.6 units) led to significant ataxic (modified Luciani), locomotor (open field) and sensorimotor (wire suspension, beam balance, inclined plane) deficits over the first week after injury ( $P < 0.05$ , Fig. 3A–F). Body weight remained stable ( $P > 0.05$ ) and most functional parameters recovered by three weeks after collagenase infusion, with the exception of inclined plane performance that showed only marginal change ( $P < 0.05$ , Fig. 3F).

### 3.4 Experiment 3: Neurocognitive Assessment at Third Week

Collagenase infused (0.6 units) animals performed significantly worse than controls across all post-operative rotarod (motor) testing blocks ( $P < 0.05$ , Fig. 4A) and were unable to improve upon their pre-operative performance ( $P > 0.05$ ), while, the controls improved their performance with each block ( $P < 0.05$ ). The T-Maze showed significant working memory differences ( $P > 0.05$ , Fig. 4B), while for the water-maze, all groups performed the cued trials (place learning) equally ( $P > 0.05$ , Fig. 4C). On the spatial blocks, however, collagenase infused animals performed significantly worse than controls ( $P < 0.05$ ), and were unable to improve upon the cued trials ( $P > 0.05$ ). As expected, the controls performed better with subsequent blocks ( $P < 0.05$ ) and with the overall spatial probe (memory trials; Fig. 4D).

### 3.5 Experiment 4: Histopathological Analysis

The topographic distribution of the lesion extended with a Gaussian distribution surrounding the level of injection at the paramedian white matter (11.6 mm caudal from bregma, Fig. 5A). The ipsilateral (right) cerebellum had an atrophic loss of brain tissue volume ( $P < 0.05$ ) without affecting the brainstem or contralateral side ( $P > 0.05$  Fig. 5B and 5C). All ventricles

remained patent and were unchanged in size ( $P>0.05$ , Fig. 5D). The cystic cavitory lesion diminished the cerebellar layers almost uniformly ( $P>0.05$ , Fig. 5E): white matter (60%  $\pm 10.6$ ), molecular (53.1%  $\pm 9.8$ ), and granular (67.8%  $\pm 14.2$ ) without any significant atrophic differences between them. Purkinje cell density was decreased bilaterally, with the greatest diminishment on the ipsilateral (peri-lesion) side ( $P<0.05$ , Fig. 5F).

#### 4. Discussion

An important translational research priority is the characterization of appropriate intracerebral hemorrhage (ICH) models (NINDS, 2005). Autologous blood or collagenase injection into the basal ganglia region of rodents represent the most common experimental approach for studying this condition (Andaluz et al., 2002; MacLellan et al., 2008; Xi et al., 2006). However, basal ganglia hemorrhage is a deep cerebral bleeding subtype, that as a group (basal ganglia, thalamus, and internal capsule), comprise no more than half of all cases (Flaherty et al., 2005), and animal models that represent the spectrum of ICH are highly needed (Gong et al., 2004; Song et al., 2007). Therefore this current study aimed to further establish a reproducible model of spontaneous cerebellar hemorrhage using stereotaxically injected collagenase (Lekic et al., 2008). This experimental paradigm could test therapeutic strategies for preventing the acutely devastating neurological deteriorations seen in patients (Jensen and St Louis, 2005; St Louis et al., 1998), and the application of cytoprotective interventions could further improve upon the lesion size and long-term neurological deficit of the survivors (Dolderer et al., 2004; Kelly et al., 2001; Okauchi et al., 2009; Strick et al., 2009; Thach, 1996).

Clinically, uncontrolled hematoma expansion (vasogenic edema and re-bleeding) will necessitate surgery in nearly half of the hospitalized cerebellar hemorrhage patients (Rosenberg and Kaufman, 1976; St Louis et al., 1998); and this infratentorial location is an independent predictor of poor prognostic outcome (Hemphill et al., 2001). The (Class I) recommendation for a surgical approach after cerebellar hemorrhage differs from ICH in all other brain regions (Broderick et al., 2007) and highlights the unique pathophysiological aspects of this cerebellar disease (Mendelow et al., 2005). *In-vitro* studies further reveal divergence of injury mechanisms when comparing cerebellar with cortical neuronal cultures (Scorziello et al., 2001). In agreement, the wide-spread use of anticoagulants has been shown to disproportionately increase the rate of hemorrhage into the cerebellum compared with other brain regions (Flaherty et al., 2006). Our cerebellar hemorrhage model is therefore especially important, since collagenase infusion effectively evaluates hemostatic mechanisms with warfarin and tPA anticoagulation (Foerch et al., 2008; Thies et al., 2004). Future experimental studies targeting hemostasis after cerebellar collagenase infusion in rats could translate into treatment strategies that improve the clinical course in conjunction with surgery (Broderick et al., 2007).

For intracerebral hemorrhage, the control of hemostasis is related both to the therapeutic approaches (Steiner and Bosel, 2010) and the propensity for injury through anticoagulant-use (Prabhakaran et al., 2010). The hemostatic findings in this study were found to stand in agreement with experimental basal ganglia ICH in rats with regards to collagenase-induced brain edema, hematoma volume, blood-brain barrier rupture, and MMP-(2 and 9) activations (Power et al., 2003; Rosenberg and Navratil, 1997; Wang and Tsirka, 2005). Although western blotting demonstrated relative changes in protein expression of these matrix-metalloproteases, the gel zymography technique better defines their enzymatic activity, and future mechanistic studies should evaluate these molecular processes further as possible venues for improving outcomes after SCH.

On the other hand, this experimental model diverged from basal ganglia ICH, in failing to produce significant 24 hour sensorimotor and ataxia deficits with the typical collagenase dose of 0.2 units (MacLellan et al., 2008). This was circumvented for the long-term studies by choosing 0.6 units of collagenase to achieve a greater initial injury. This dose approximates that which was shown to avoid neurotoxicity in rodents (Matsushita et al., 2000), although cell death appears to be a less significant factor after cerebellar hemorrhage as compared to most other brain regions (Qureshi et al., 2003).

Collagenase infusion (0.6 units) yielded long-term neurobehavioral patterns that were very analogous with clinical reports after cerebellar hemorrhage in humans. Our study demonstrated that most neurological impairments resolved over the first three weeks of assessments, while motor-learning (rotarod) and cognitive ability (water-maze) remained impaired at one month after injury. In agreement, almost one-half of survivors from cerebellar hemorrhage will retain long-term deficits across motor-learning and visuospatial neurocognitive domains, even after full rehabilitation from ataxic losses of coordination, muscle tone, and overall strength (Baillieux et al., 2008; Dolderer et al., 2004; Kelly et al., 2001; Strick et al., 2009). On the other hand, our finding of marginal hind-limb recovery (inclined plane) was divergent from these clinical manifestations. This is possibly a rodent-specific feature, due to the central placement of our cerebellar lesion that anatomically occupies the hind-limb control region; while the forelimb neurons are located more peripherally in the rodent cerebellum (Peeters et al., 1999). Future studies should apply therapeutic strategies, while extending the later neurobehavioral time-points, to better determine the reversibility of hind-limb function, cognitive ability and for translational application (Hua et al., 2006).

Neurobehavioral outcomes need to be correlated to a histopathological lesion, as a morphological measure of brain injury (Felberg et al., 2002; Hua et al., 2002). The cerebellum is organized into a geometric lattice with one-tenth the cerebral cortical volume, but four times the neuronal amount (Andersen et al., 1992). Thirty days after collagenase infusion, we found a well circumscribed cystic-cavitary lesion within the right cerebellum. The atrophy was focal and did not affect the contralateral side, similar to basal ganglia hemorrhage using rats (MacLellan et al., 2008). There also wasn't any difference between percent atrophy of the individual cerebellar layers; however, the early contralateral spreading of edema was followed by a bilateral loss in Purkinje cell density one month later. Since Purkinje cells are the primary output of the cerebellum (Baillieux et al., 2008), this neuronal group could be an additional contributor to the cognitive deficits in addition to the atrophic lesion alone. Taken together, these neuronal tissue losses represent a huge opportunity for neuroprotection strategies.

Cerebellar stroke is a human disease where clinical symptoms can be mapped to an acute lesion in a previously healthy cerebellum. In the past, these clinical cases have allowed investigators to better understand the functional and morphological aspects of cerebellar recovery (Timmann et al., 2009). To date, rats undergoing hemicerebellectomy (HCb) had been the experimental correlates to this clinical cerebellar injury paradigm (Leggio et al., 2000). As an extension, our results indicate that collagenase infusion produces a lasting focal lesion and neurobehavioral profiles similar to cerebellar stroke patients. This approach overcomes several complications associated with rodent HCb, such as animal mortality and profound weight loss (Colombel et al., 2002). Therefore, future applications of collagenase infusion can have broad translational implications for cerebellar study.

## 5. Conclusion

We have characterized the early brain injury, neurobehavioral profiles, and histopathology in a highly reliable and easily reproducible experimental model of cerebellar hemorrhage in rats. Therapeutic strategies that mitigate the mass effect (brain edema and hematoma growth) and promote lasting neuroprotection (neurobehavioral and atrophic recovery) could lead to clinical approaches that afford these patients better outcomes in the future (Qureshi et al., 2009; Xi et al., 2006). These findings therefore provide a basis for characterizing the pathophysiological features of this disease, and establish a foundation for performing further preclinical therapeutic investigation.

### Highlight

Spontaneous cerebellar hemorrhage (SCH) represents approximately 10% of all intracerebral hemorrhage (ICH), and is an important clinical problem of which little is known. This study established a new animal model of intracerebellar hemorrhage in rats.

Early neurological deficits including brain water, hemoglobin assay, Evans blue, collagen-IV, ZO-1, and MMP-2 and MMP-9 were measured to support brain injury after cerebellar hemorrhage observed clinically.

Long term neurological and neurobehavioral functional evaluations over thirty days were conducted including the ataxia scale (modified Luciani), open field, wire suspension, beam balance and inclined plane (Experiment 2) to verify cerebellar injury in this new model.

Cerebellar hemorrhage is an under studied area and this animal model to help to promote experimental studies of cerebellar hemorrhage.

## Supplementary Material

Refer to Web version on PubMed Central for supplementary material.

## Acknowledgments

This study was partially supported by a grant (NS053407) from the National Institutes of Health to J.H.Z.

## References

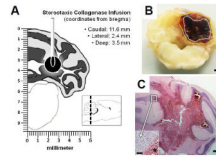
1. Andaluz N, Zuccarello M, Wagner KR. Experimental animal models of intracerebral hemorrhage. *Neurosurg Clin N Am* 2002;13:385–393. [PubMed: 12486927]
2. Andersen BB, Korbo L, Pakkenberg B. A quantitative study of the human cerebellum with unbiased stereological techniques. *J Comp Neurol* 1992;326:549–560. [PubMed: 1484123]
3. Baillieux H, De Smet HJ, Paquier PF, De Deyn PP, Marien P. Cerebellar neurocognition: insights into the bottom of the brain. *Clin Neurol Neurosurg* 2008;110:763–773. [PubMed: 18602745]
4. Broderick J, Connolly S, Feldmann E, Hanley D, Kase C, Krieger D, Mayberg M, Morgenstern L, Ogilvy CS, Vespa P, Zuccarello M. Guidelines for the management of spontaneous intracerebral hemorrhage in adults: 2007 update: a guideline from the American Heart Association/American Stroke Association Stroke Council, High Blood Pressure Research Council, and the Quality of Care and Outcomes in Research Interdisciplinary Working Group. *Stroke* 2007;38:2001–2023. [PubMed: 17478736]
5. Choudhri TF, Hoh BL, Solomon RA, Connolly ES Jr, Pinsky DJ. Use of a spectrophotometric hemoglobin assay to objectively quantify intracerebral hemorrhage in mice. *Stroke* 1997;28:2296–2302. [PubMed: 9368579]



6. Colombel C, Lalonde R, Caston J. The effects of unilateral removal of the cerebellar hemispheres on motor functions and weight gain in rats. *Brain Res* 2002;950:231–238. [PubMed: 12231248]
7. Cossu M, Dorcaratto A, Pau A, Rodriguez G, Sehrbunt Viale E, Siccardi D, Viale GL. Changes in infratentorial blood flow following experimental cerebellar haemorrhage. preliminary report. *Ital J Neurol Sci* 1991;12:69–73. [PubMed: 1757226]
8. Cossu M, Pau A, Siccardi D, Viale GL. Infratentorial ischaemia following experimental cerebellar haemorrhage in the rat. *Acta Neurochir (Wien)* 1994;131:146–150. [PubMed: 7709777]
9. Dolderer S, Kallenberg K, Aschoff A, Schwab S, Schwarz S. Long-term outcome after spontaneous cerebellar haemorrhage. *Eur Neurol* 2004;52:112–119. [PubMed: 15319556]
10. Fathali N, Ostrowski RP, Lekic T, Jadhav V, Tong W, Tang J, Zhang JH. Cyclooxygenase-2 inhibition provides lasting protection against neonatal hypoxic-ischemic brain injury. *Crit Care Med* 2010;38:572–578. [PubMed: 20029340]
11. Felberg RA, Grotta JC, Shirzadi AL, Strong R, Narayana P, Hill-Felberg SJ, Aronowski J. Cell death in experimental intracerebral hemorrhage: the "black hole" model of hemorrhagic damage. *Ann Neurol* 2002;51:517–524. [PubMed: 11921058]
12. Fernandez AM, de la Vega AG, Torres-Aleman I. Insulin-like growth factor I restores motor coordination in a rat model of cerebellar ataxia. *Proc Natl Acad Sci U S A* 1998;95:1253–1258. [PubMed: 9448318]
13. Flaherty ML, Haverbusch M, Sekar P, Kissela B, Kleindorfer D, Moomaw CJ, Sauerbeck L, Schneider A, Broderick JP, Woo D. Long-term mortality after intracerebral hemorrhage. *Neurology* 2006;66:1182–1186. [PubMed: 16636234]
14. Flaherty ML, Haverbusch M, Sekar P, Kissela BM, Kleindorfer D, Moomaw CJ, Broderick JP, Woo D. Location and outcome of anticoagulant-associated intracerebral hemorrhage. *Neurocrit Care* 2006;5:197–201. [PubMed: 17290088]
15. Flaherty ML, Woo D, Haverbusch M, Sekar P, Khoury J, Sauerbeck L, Moomaw CJ, Schneider A, Kissela B, Kleindorfer D, Broderick JP. Racial variations in location and risk of intracerebral hemorrhage. *Stroke* 2005;36:934–937. [PubMed: 15790947]
16. Foerch C, Arai K, Jin G, Park KP, Pallast S, van Leyen K, Lo EH. Experimental model of warfarin-associated intracerebral hemorrhage. *Stroke* 2008;39:3397–3404. [PubMed: 18772448]
17. Gong Y, Hua Y, Keep RF, Hoff JT, Xi G. Intracerebral hemorrhage: effects of aging on brain edema and neurological deficits. *Stroke* 2004;35:2571–2575. [PubMed: 15472083]
18. Hartman R, Lekic T, Rojas H, Tang J, Zhang JH. Assessing functional outcomes following intracerebral hemorrhage in rats. *Brain Res* 2009;1280:148–157. [PubMed: 19464275]
19. Hemphill JC 3rd, Bonovich DC, Besmertis L, Manley GT, Johnston SC. The ICH score: a simple, reliable grading scale for intracerebral hemorrhage. *Stroke* 2001;32:891–897. [PubMed: 11283388]
20. Hill MD, Silver FL. Epidemiologic predictors of 30-day survival in cerebellar hemorrhage. *J Stroke Cerebrovasc Dis* 2001;10:118–121. [PubMed: 17903811]
21. Hua Y, Nakamura T, Keep RF, Wu J, Schallert T, Hoff JT, Xi G. Long-term effects of experimental intracerebral hemorrhage: the role of iron. *J Neurosurg* 2006;104:305–312. [PubMed: 16509506]
22. Hua Y, Schallert T, Keep RF, Wu J, Hoff JT, Xi G. Behavioral tests after intracerebral hemorrhage in the rat. *Stroke* 2002;33:2478–2484. [PubMed: 12364741]
23. Hughes RN. The value of spontaneous alternation behavior (SAB) as a test of retention in pharmacological investigations of memory. *Neurosci Biobehav Rev* 2004;28:497–505. [PubMed: 15465137]
24. Jensen MB, St Louis EK. Management of acute cerebellar stroke. *Arch Neurol* 2005;62:537–544. [PubMed: 15824250]
25. Kelly PJ, Stein J, Shafiqat S, Eskey C, Doherty D, Chang Y, Kurina A, Furie KL. Functional recovery after rehabilitation for cerebellar stroke. *Stroke* 2001;32:530–534. [PubMed: 11157193]
26. Korbo L, Andersen BB, Ladefoged O, Moller A. Total numbers of various cell types in rat cerebellar cortex estimated using an unbiased stereological method. *Brain Res* 1993;609:262–268. [PubMed: 8508308]

27. Leggio MG, Molinari M, Neri P, Graziano A, Mandolesi L, Petrosini L. Representation of actions in rats: the role of cerebellum in learning spatial performances by observation. *Proc Natl Acad Sci U S A* 2000;97:2320–2325. [PubMed: 10681456]
28. Lekic T, Hartman R, Rojas H, Manaenko A, Chen W, Ayer R, Tang J, Zhang JH. Protective effect of melatonin upon neuropathology, striatal function, and memory ability after intracerebral hemorrhage in rats. *J Neurotrauma* 2010;27:627–637. [PubMed: 20350200]
29. Lekic T, Tang J, Zhang JH. Rat model of intracerebellar hemorrhage. *Acta Neurochir Suppl* 2008;105:131–134. [PubMed: 19066098]
30. MacLellan CL, Silasi G, Poon CC, Edmundson CL, Buist R, Peeling J, Colbourne F. Intracerebral hemorrhage models in rat: comparing collagenase to blood infusion. *J Cereb Blood Flow Metab* 2008;28:516–525. [PubMed: 17726491]
31. Matsushita K, Meng W, Wang X, Asahi M, Asahi K, Moskowitz MA, Lo EH. Evidence for apoptosis after intercerebral hemorrhage in rat striatum. *J Cereb Blood Flow Metab* 2000;20:396–404. [PubMed: 10698078]
32. Mendelow AD, Gregson BA, Fernandes HM, Murray GD, Teasdale GM, Hope DT, Karimi A, Shaw MD, Barer DH. Early surgery versus initial conservative treatment in patients with spontaneous supratentorial intracerebral haematomas in the International Surgical Trial in Intracerebral Haemorrhage (STICH): a randomised trial. *Lancet* 2005;365:387–397. [PubMed: 15680453]
33. Mendelow AD, Unterberg A. Surgical treatment of intracerebral haemorrhage. *Curr Opin Crit Care* 2007;13:169–174. [PubMed: 17327738]
34. NINDS. Priorities for clinical research in intracerebral hemorrhage: report from a National Institute of Neurological Disorders and Stroke workshop. *Stroke* 2005;36:e23–e41. [PubMed: 15692109]
35. Okauchi M, Hua Y, Keep RF, Morgenstern LB, Xi G. Effects of deferoxamine on intracerebral hemorrhage-induced brain injury in aged rats. *Stroke* 2009;40:1858–1863. [PubMed: 19286595]
36. Oorschot DE. Total number of neurons in the neostriatal, pallidal, subthalamic, and substantia nigral nuclei of the rat basal ganglia: a stereological study using the cavalieri and optical disector methods. *J Comp Neurol* 1996;366:580–599. [PubMed: 8833111]
37. Peeters RR, Verhoye M, Vos BP, Van Dyck D, Van Der Linden A, De Schutter E. A patchy horizontal organization of the somatosensory activation of the rat cerebellum demonstrated by functional MRI. *Eur J Neurosci* 1999;11:2720–2730. [PubMed: 10457168]
38. Power C, Henry S, Del Bigio MR, Larsen PH, Corbett D, Imai Y, Yong VW, Peeling J. Intracerebral hemorrhage induces macrophage activation and matrix metalloproteinases. *Ann Neurol* 2003;53:731–742. [PubMed: 12783419]
39. Prabhakaran S, Rivolta J, Vieira JR, Rincon F, Stillman J, Marshall RS, Chong JY. Symptomatic Intracerebral Hemorrhage Among Eligible Warfarin-Treated Patients Receiving Intravenous Tissue Plasminogen Activator for Acute Ischemic Stroke. *Arch Neurol*. 2010
40. Qureshi AI, Mendelow AD, Hanley DF. Intracerebral haemorrhage. *Lancet* 2009;373:1632–1644. [PubMed: 19427958]
41. Qureshi AI, Suri MF, Ostrow PT, Kim SH, Ali Z, Shatla AA, Guterman LR, Hopkins LN. Apoptosis as a form of cell death in intracerebral hemorrhage. *Neurosurgery* 2003;52:1041–1047. discussion 1047–1048. [PubMed: 12699545]
42. Rosenberg GA, Kaufman DM. Cerebellar hemorrhage: reliability of clinical evaluation. *Stroke* 1976;7:332–336. [PubMed: 1085507]
43. Rosenberg GA, Mun-Bryce S, Wesley M, Kornfeld M. Collagenase-induced intracerebral hemorrhage in rats. *Stroke* 1990;21:801–807. [PubMed: 2160142]
44. Rosenberg GA, Navratil M. Metalloproteinase inhibition blocks edema in intracerebral hemorrhage in the rat. *Neurology* 1997;48:921–926. [PubMed: 9109878]
45. Saria A, Lundberg JM. Evans blue fluorescence: quantitative and morphological evaluation of vascular permeability in animal tissues. *J Neurosci Methods* 1983;8:41–49. [PubMed: 6876872]
46. Schmidt WM, Kraus C, Hoyer H, Hochmeister S, Oberndorfer F, Branka M, Bingemann S, Lassmann H, Muller M, Macedo-Souza LI, Vainzof M, Zatz M, Reis A, Bittner RE. Mutation in the *Scyl1* gene encoding amino-terminal kinase-like protein causes a recessive form of spinocerebellar neurodegeneration. *EMBO Rep* 2007;8:691–697. [PubMed: 17571074]

47. Scorziello A, Pellegrini C, Forte L, Tortiglione A, Gioielli A, Iossa S, Amoroso S, Tufano R, Di Renzo G, Annunziato L. Differential vulnerability of cortical and cerebellar neurons in primary culture to oxygen glucose deprivation followed by reoxygenation. *J Neurosci Res* 2001;63:20–26. [PubMed: 11169610]
48. Song S, Hua Y, Keep RF, Hoff JT, Xi G. A new hippocampal model for examining intracerebral hemorrhage-related neuronal death: effects of deferoxamine on hemoglobin-induced neuronal death. *Stroke* 2007;38:2861–2863. [PubMed: 17761912]
49. St Louis EK, Wijdicks EF, Li H. Predicting neurologic deterioration in patients with cerebellar hematomas. *Neurology* 1998;51:1364–1369. [PubMed: 9818861]
50. Steiner T, Bosel J. Options to restrict hematoma expansion after spontaneous intracerebral hemorrhage. *Stroke* 2010;41:402–409. [PubMed: 20044536]
51. Strick PL, Dum RP, Fiez JA. Cerebellum and nonmotor function. *Annu Rev Neurosci* 2009;32:413–434. [PubMed: 19555291]
52. Tang J, Liu J, Zhou C, Alexander JS, Nanda A, Granger DN, Zhang JH. Mmp-9 deficiency enhances collagenase-induced intracerebral hemorrhage and brain injury in mutant mice. *J Cereb Blood Flow Metab* 2004;24:1133–1145. [PubMed: 15529013]
53. Thach WT. On the specific role of the cerebellum in motor learning and cognition: Clues from PET activation and lesion studies in man. *Behav. Brain Sci* 1996;19:411–431.
54. Thiex R, Mayfrank L, Rohde V, Gilsbach JM, Tsirka SA. The role of endogenous versus exogenous tPA on edema formation in murine ICH. *Exp Neurol* 2004;189:25–32. [PubMed: 15296833]
55. Timmann D, Konczak J, Ilg W, Donchin O, Hermsdorfer J, Gizewski ER, Schoch B. Current advances in lesion-symptom mapping of the human cerebellum. *Neuroscience* 2009;162:836–851. [PubMed: 19409233]
56. Wang J, Tsirka SE. Neuroprotection by inhibition of matrix metalloproteinases in a mouse model of intracerebral haemorrhage. *Brain* 2005;128:1622–1633. [PubMed: 15800021]
57. Xi G, Keep RF, Hoff JT. Mechanisms of brain injury after intracerebral haemorrhage. *Lancet Neurol* 2006;5:53–63. [PubMed: 16361023]
58. Zhou Y, Fathali N, Lekic T, Tang J, Zhang JH. Glibenclamide improves neurological function in neonatal hypoxia-ischemia in rats. *Brain Res* 2009;1270:131–139. [PubMed: 19306849]

**Fig.1. Experimental Model of Cerebellar Hemorrhage**

(A) Schematic showing stereotaxic needle placement into the right paramedian white matter (inset demonstrating sagittal view with dotted-line at craniocaudal level). (B) Photograph of coronal section showing the hematoma surrounded by vasogenic edema at 24 hours after collagenase (0.6 units) infusion (outlined with dotted lines, bar= 1 mm) and (C) a representative H&E-stained cryosection illustrating hematoma location (bar= 0.5 mm) with inset showing hematoma (\*) border (bar= 20 µm).

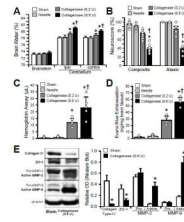


**Fig.2. Early Brain Injury at 24 Hours**

(A) Brain Water, (B) Neuroscore, (C) Hematoma Volume, (D) Vascular Permeability, and (E) Immunoblots (left) with semi-quantification (right) for Collagen-IV, ZO-1, MMP-2 and MMP-9. The values are expressed as mean  $\pm$ SEM, n= 10 (neuroscore) and n= 5 (all others), \* $P$ <0.05 compared with controls (sham and needle trauma), † $P$ <0.05 compared with collagenase infusion (0.2 units).

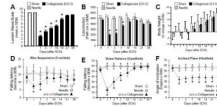


**Fig.3. Functional Outcome over Thirty Days**

(A) Luciani Ataxia Scale, (B) Locomotion, (C) Body Weight, (D) Wire Suspension, (E) Beam Balance, (F) Inclined Plane. The values are expressed as mean  $\pm$ SEM, n=8 (per group), \* $P$ <0.05 is comparing collagenase infusion (0.6 units, closed triangles) with controls (sham and needle trauma, open circles).

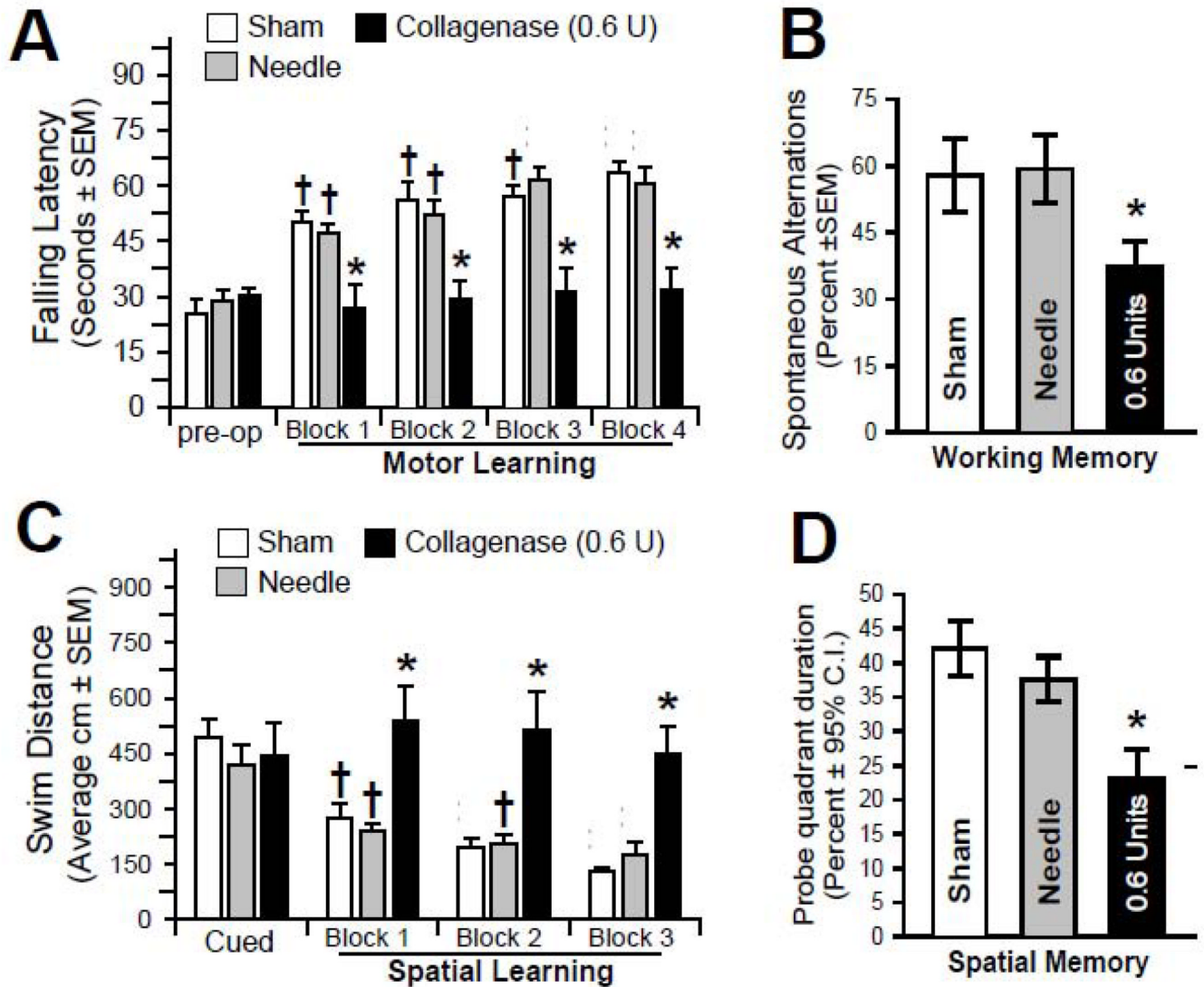


**Fig.4. Neurocognitive Assessment at Third Week**

(A) Motor learning was assessed by the change in the latency to fall off an accelerating rotarod (2 rpm/ 5 sec) preoperatively and across four daily blocks. (B) Working memory was quantified by the number of spontaneous alternations in the T-Maze. (C) Spatial learning was assessed by the swim distance needed to find the visible (cued) versus the hidden (spatial) platforms in the water-maze. (D) Spatial memory was determined by the percent duration in the probe quadrant when the platform was removed. The values are expressed as mean  $\pm$ SEM (rotarod, cued and spatial water-maze) and mean  $\pm$ 95th C.I. (probe quadrant),  $n=8$  (per group),  $*P<0.05$  compared with controls (sham and needle trauma),  $\dagger P<0.05$  compared with pre-operation (rotarod) or cued trials (spatial water-maze), and  $\ddagger P<0.05$  compared with Block 1 (rotarod and spatial water-maze)

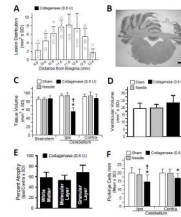


**Fig.5. Histopathological Analysis**

(A) Lesion distribution (mm<sup>2</sup>) over the right cerebellar hemisphere. (B) Representative cryosection illustrating the cystic-cavitory lesion (scale bar= 1 mm). (C) Infratentorial brain tissue volume (mm<sup>3</sup>). (D) Volume of the ventricles (mm<sup>3</sup>). (E) Percent atrophy of white matter, molecular layer and granular layer, expressed as the volumetric difference between ipsilateral and contralateral folia. (F) Purkinje cell counts per millimeter (mm) over the intact (non-lesioned) areas of the cerebellum. Values expressed as mean  $\pm$ SD, n=8 (per group), DCN indicates deep cerebellar nuclei, \* $P$ <0.05 compared with controls (sham and needle), † $P$ <0.05 compared with contralateral side (tissue volume and purkinje cells).



Table 1

Arterial Blood Gas analysis (pH, PO<sub>2</sub>, PCO<sub>2</sub>), Mean Arterial Blood Pressure (BP), Heart Rate (HR), and Blood Glucose (BG) during and after (30 Min and 24 Hr) Collagenase Infusion (C.I.)

Group	pH	PO <sub>2</sub> (mm Hg)	PCO <sub>2</sub> (mm Hg)	BP (mm Hg)	HR (per min)	BG (mg/dL)
During C.I.						
Sham	7.33±0.03	184±35	45±3	82±6	338±40	209±62
Needle	7.36±0.03	184±21	42±4	90±7	357±16	245±69
C.I.—0.2 Units	7.33±0.10	187±17	43±7	93±7	366±42	212±42
C.I.—0.6 Units	7.34±0.09	192±43	45±12	93±9	372±28	217±50
30 Min after C.I.						
Sham	7.32±0.01	186±19	47±3	83±6	344±24	218±38
Needle	7.34±0.01	185±12	43±1	87±8	350±18	191±49
C.I.—0.2 Units	7.33±0.08	193±25	42±6	91±5	355±17	180±35
C.I.—0.6 Units	7.31±0.11	199±41	46±9	91±10	365±25	223±51
24 Hr after C.I.						
Sham	7.5±0.04	192±12	36±5	84±5	348±20	229±15
Needle	7.51±0.05	180±16	37±7	85±8	359±33	192±12
C.I.—0.2 Units	7.51±0.04	189±5	34±3	81±5	347±23	197±21
C.I.—0.6 Units	7.53±0.04	188±55	34±7	83±4	365±33	206±54

Values are mean ± SD. No significant differences among groups.